Atmos. Chem. Phys. Discuss., 9, 24783–24814, 2009
www.atmos-chem-phys-discuss.net/9/24783/2009/

Atmospheric Chemistry and Physics Discussions

This discussion paper is/has been under review for the journal Atmospheric Chemistry and Physics (ACP). Please refer to the corresponding final paper in ACP if available.

Tropospheric photooxidation of CF_3CH_2CHO and $CF_3(CH_2)_2CHO$ initiated by Cl atoms and OH radicals

M. Antiñolo[1], E. Jiménez[1], A. Notario[2], E. Martínez[1], and J. Albaladejo[1]

[1]Departamento de Química Física, Facultad de Ciencias Químicas. Universidad de Castilla-La Mancha. Avda. Camilo José Cela, s/n. 13071 Ciudad Real, Spain
[2]Instituto de Tecnologías Química y Medioambiental (ITQUIMA). Universidad de Castilla-La Mancha, Avda. Camilo José Cela, s/n. 13071 Ciudad Real, Spain

Received: 7 October 2009 – Accepted: 8 October 2009 – Published: 19 November 2009

Correspondence to: J. Albaladejo (jose.albaladejo@uclm.es)

Published by Copernicus Publications on behalf of the European Geosciences Union.

Abstract

The absolute rate coefficients for the tropospheric reactions of chlorine (Cl) atoms and hydroxyl (OH) radicals with CF_3CH_2CHO and $CF_3(CH_2)_2CHO$ were measured as a function of temperature (263–371 K) and pressure (50–215 Torr of He) by pulsed UV laser photolysis techniques. Vacuum UV resonance fluorescence was employed to detect and monitor the time evolution of Cl atoms. Laser induced fluorescence was used in this work as a detection of OH radicals as a function of reaction time. No pressure dependence of the bimolecular rate coefficients, k_{Cl} and k_{OH}, was found at all temperatures. At room temperature k_{Cl} and k_{OH} were (in 10^{-11} cm^3 molecule^{-1} s^{-1}): $k_{Cl}(CF_3CH_2CHO) = (1.55\pm0.53)$; $k_{Cl}(CF_3(CH_2)_2CHO) = (3.39\pm1.38)$; $k_{OH}(CF_3CH_2CHO) = (0.259\pm0.050)$; $k_{OH}(CF_3(CH_2)_2CHO) = (1.28\pm0.24)$. A slightly negative temperature dependence of k_{Cl} was observed for CF_3CH_2CHO and $CF_3(CH_2)_2CHO$, and $k_{OH}(CF_3CH_2CHO)$. In contrast, $k_{OH}(CF_3(CH_2)_2CHO)$ did not exhibit a temperature dependence in the studied ranged. Arrhenius expressions for these reactions were:

$$k_{Cl}(CF_3CH_2CHO) = (4.4\pm1.0)\times10^{-11}\exp\{-(316\pm68)/T\}\,\mathrm{cm^3\,molecule^{-1}\,s^{-1}},$$

$$k_{Cl}(CF_3(CH_2)_2CHO) = (2.9\pm0.7)\times10^{-10}\exp\{-(625\pm80)/T\}\,\mathrm{cm^3\,molecule^{-1}\,s^{-1}},$$

$$k_{OH}(CF_3CH_2CHO) = (7.8\pm2.2)\times10^{-12}\exp\{-(314\pm90)/T\}\,\mathrm{cm^3\,molecule^{-1}\,s^{-1}}.$$

The atmospheric impact of the homogeneous removal by OH radicals and Cl atoms of these fluorinated aldehydes is discussed in terms of the global atmospheric lifetimes, taking into account different degradation pathways. The calculated lifetimes show that atmospheric oxidation of $CF_3(CH_2)_xCHO$ are globally dominated by OH radicals, however reactions initiated by Cl atoms can act as a source of free radicals at dawn in the troposphere.

ACPD

9, 24783–24814, 2009

1 Introduction

The only long term solution to solve the problem of the depletion of the ozone layer is to phase out the use of chlorofluorocarbons (CFCs) and to substitute them by other family of compounds with lower or zero Ozone Depletion Potential (ODP). Initially, among the candidates for replacing CFCs were the hydrofluorocarbons (HFCs) and hydrochlorofluorocarbons (HCFCs) (Atkinson et al., 1989). But, although HFCs have a zero ODP, HCFCs do affect stratospheric ozone because of the presence of chlorine atoms in these species. Moreover, both of them are very strong greenhouse gases with high Global Warming Potentials (GWP) due to the long tropospheric lifetimes and strong absorption in the IR region. Recently, hydrofluoroethers (HFEs) and partially fluorinated alcohols, like the family of $CF_3(CH_2)_xCH_2OH$, have been suggested as alternatives for HFCs and HCFCs.

CF_3CH_2OH and $CF_3CH_2CH_2OH$ have negligible GWPs (Sellevåg et al., 2004a; Waterland et al., 2005) and a zero ODP, since the CF_3 group does not cause significant ozone depletion (Ravishankara et al., 1994). On the other hand, atmospheric photooxidation of these fluorinated alcohols, initiated by hydroxyl (OH) radicals and chlorine (Cl) atoms, is known to yield fluorinated aldehydes as major products (Kelly et al., 2005; Hurley et al., 2004, 2005; Sellevåg et al., 2004a). Therefore, a complete understanding of the atmospheric fate of $CF_3(CH_2)_xCHO$ would be needed in order to better evaluate the environmental implications of these hydrofluoroalcohols as CFCs substitutes.

As far as we know, only kinetic studies on the reactions of CF_3CHO and CF_3CH_2CHO with the main oxidizing agents in the atmosphere, OH radicals and Cl atoms, have been reported almost exclusively by relative rate methods at room temperature (Atkinson et al., 2008; Kelly et al., 2005; Hurley et al., 2005; Sellevåg et al., 2004b). Neither OH and Cl kinetic data on other trifluoroaldehydes nor kinetic data on the reactions with NO_3 and O_3 were found in the literature. So, the aim of this work is to determine the absolute rate coefficients for the OH- and Cl-reaction with 3,3,3-trifluoropropanal (CF_3CH_2CHO) and 4,4,4-trifluorobutanal ($CF_3(CH_2)_2CHO$) as

ACPD
9, 24783–24814, 2009

a function of temperature (T =263–371 K):

$$Cl + CF_3(CH_2)_xCHO \rightarrow \text{Products} \quad k_{Cl} \tag{1}$$

$$OH + CF_3(CH_2)_xCHO \rightarrow \text{Products} \quad k_{OH} \tag{2}$$

Pulsed Laser Photolysis (PLP) techniques were employed in this work to generate the transient species, Cl atoms and OH radicals, which were detected and monitored by Resonance Fluorescence (RF) and Laser Induced Fluorescence (LIF), respectively. An expression for the temperature dependence of k_{Cl} and k_{OH} is recommended in this paper, which allows the derivation of the rate coefficients, and the corresponding lifetime due to the homogeneous removal, for all reactions at tropospheric temperatures. The possible atmospheric impact of these secondary pollutants will be discussed in terms of their gas-phase reactivity and other degradation routes.

2 Experimental and procedure

Kinetic measurements on the set of Reactions (1) and (2) have been performed by UV laser pulsed photolysis techniques described earlier (Albaladejo et al., 2002, 2003; Jiménez et al., 2005, 2007). A brief description of the PLP/RF experimental set-up is given in Sect. 2.1. The PLP/ LIF experimental system, described briefly in Sect. 2.2, was modified in order to measure in situ the fluoroaldehyde concentration. A detailed description of this latter set-up is presented in Sect. 2.3. Analysis procedure of the kinetic data is described in Sect. 2.4.

2.1 Cl kinetics: PLP/RF system

A Pyrex jacketed reaction cell with an internal volume of about 200 cm^3 was employed in the kinetic measurements of Reaction (R1) as a function of temperature. Cl atoms

were produced by the photolysis of Cl_2 ($(2.1-3.7)\times10^{14}$ molecule cm^{-3}) at 308 nm using a pulsed XeCl excimer laser (Lambda Physik LPX 105i). The concentration of Cl atoms was monitored as a function of time by resonance fluorescence at $\lambda\sim135$ nm. Ground state Cl($^3P_{3/2}$) was excited by the 135 nm radiation from a microwave-driven lamp, situated perpendicular to the photolysis laser beam, through which He containing a low concentration of Cl_2 (0.2–0.3%) was flowed. The resonance fluorescence (RF) radiation was recorded with a solar blind photomultiplier, PMT (Hamamatsu R6835) positioned perpendicular to both the resonance lamp and photolysis laser beam, after passing through two CaF_2 lenses. The regions between the two lenses and between the last lens and the photomultiplier were pumped in order to remove ambient O_2, which absorbs the RF at 135 nm.

Signals were obtained using photon counting electronics and multichannel scaling data storage. The output signal from the PMT was first input into a fast preamplifier and then collected with a multichannel scaler (EG&G Instruments T914P) and stored in a coupled microcomputer for subsequent analysis. Data acquisition by the multichannel scaler was triggered between 0.1 ms and 10 ms (ca. 10% of the total temporal scale) prior to the photolysis laser in order to obtain the background signal which was subtracted from the post photolysis signal to obtain the temporal profile of the Cl atoms. The Cl temporal profiles following 5000 to 30 000 laser pulses were coadded to improve the signal-to-noise ratio.

All experiments were carried out in a large excess of buffer gas (He). Diluted fluoroaldehydes and Cl_2/He mixtures were slowly flowed from 10-L bulbs into the reaction cell by means of electronic mass flow controllers. Concentrations of the different gases were measured from their mass flow rates and the total pressure. The flow rate (180–300 sccm) was fast enough to prevent the accumulation of photolysis or reaction products, but slow enough for considering the mixture static during the measurements.

ACPD
9, 24783–24814, 2009

2.2 OH kinetics: PLP/LIF system

A schematics of the experimental set-up modified for this work is shown in Fig. 1. The Pyrex reaction cell was identical to that used in the Cl kinetics. OH($X^2\Pi$) radicals were generated by the pulsed photolysis of H_2O_2(g) at 248 nm by using a KrF excimer laser. Gas-phase H_2O_2 was introduced in the reaction cell by bubbling the carrier gas (He) through a pre-concentrated liquid sample of hydrogen peroxide (Jiménez et al., 2005). Upper limits for H_2O_2 concentrations in the reaction cell, were estimated as described in our previous paper (Jiménez et al., 2007), and were in the range of $(0.7–4.8)\times10^{14}$ molecule cm^{-3}. Therefore, OH concentration can be estimated from the upper limit of the H_2O_2 concentration, taking into account the absorption cross section of H_2O_2 at 248 nm, the quantum yield for OH production (Sander et al., 2006), and the photolysis laser fluence ((2.0–8.4) mJ pulse^{-1} cm^{-2}). OH radical concentration was around 3.0×10^{11} molecule cm^{-3} in all experiments. At different reaction times, OH radicals were excited at 282 nm (OH($A^2\Sigma^+, v'=1$)←OH($X^2\Pi, v''=0$)) by using the frequency-doubled output of a dye laser pumped by a Nd-YAG laser. LIF signal from OH($A^2\Sigma^+$) was detected at $\lambda\geq282$ nm by a photomultiplier tube placed orthogonal to both light sources. LIF emissions were selected by a bandpass filter (90% transmittance at 350 nm and 150 nm of FWHM) and transferred to a personal computer for analysis.

2.3 Optically measurement of [$CF_3(CH_2)_xCHO$]

An accurate measurement of $CF_3(CH_2)_xCHO$ concentrations is essential to report a rate coefficient within reasonable quoted uncertainties. As in our previous works (Jiménez et al., 2005, 2007; Lanza et al., 2008), firstly, the absorption cross sections at 185 nm ($\sigma_{\lambda=185nm}$) were measured in order to use them in the determination of reactant concentrations during the kinetic experiments. These experiments were conducted at pressures inside the absorption cell between 0.2 and 8.4 Torr of pure fluorinated aldehydes. $\sigma_{\lambda=185nm}$ were obtained from the slope of the plots of absorbance (in base

ACPD
9, 24783–24814, 2009

e) versus pressure and using a large number of experiments (30 runs). $\sigma_{\lambda=185nm}$ were found to be $(4.82\pm0.20)\times10^{-20}$ cm^2 molecule^{-1} and $(9.42\pm0.19)\times10^{-20}$ cm^2 molecule^{-1} for CF_3CH_2CHO and $CF_3(CH_2)_2CHO$, respectively. The stated uncertainty was $\pm2\sigma$ (only statistical error). Some examples of the Beer-Lambert plots are given in Fig. 1S of the supplementary information for both aldehydes. The low absorption cross section (almost three orders of magnitude lower than non-fluorinated aldehydes) did not allow the measurement of aldehyde concentrations during the kinetic experiments, since the decrease in the intensity of the incident radiation was not measurable (absorbances much lower than 0.1%).

For that reason, concentrations of $CF_3(CH_2)_xCHO$ were measured in situ during the kinetic experiments by Fourier transform infrared (FTIR) spectroscopy, mainly at the exit of the reaction cell, by using the experimental set-up presented in Fig. 1. Some experiments $CF_3(CH_2)_xCHO$ concentration was measured before entering the reaction cell and no difference outside the experimental error was observed. These concentration measurements were performed in a borosilicate glass multipass cell of variable path length from 1 to 8 m (Specac, Cyclone C5) sealed with ZnSe windows (transmittance range: 450–17 000 cm^{-1}). The FTIR cell is provided with protected gold mirrors and vacuum/gas inlet and outlet taps. The path length was set by means of a low power diode laser (0.8 mW at 635 nm) (Specac, P/N 24500 Benchmark™ Series Laser Alignment Accessory). All experiments were performed with a fixed pathlength of 8 m. A FTIR spectrometer (Bruker, TENSOR 27), with a cube corner interferometer which eliminates the alignment errors, was used to record the FTIR spectra of both aldehydes. A N_2-liquid cooled mercury cadmium telluride (MCT) detector was used during the quantification process. The FTIR spectra of diluted fluorinated aldehydes during the calibration were recorded at a total pressure between 1.3 and 96 Torr in He. The dilution factors in the storage bulbs, f, defined as $f = pCF_3(CH_2)_xCHO/\{pCF_3(CH_2)_xCHO + pHe\}$, ranged from 1×10^{-4} to 8.3×10^{-3}.

An example of the FTIR spectrum range of diluted CF_3CH_2CHO and $CF_3(CH_2)_2CHO$ and recorded in the 500–4000 cm^{-1} region is shown in Fig. 2S of the supplementary in-

formation. The four absorption bands used in the quantification of the fluorinated aldehydes during the kinetic experiment are listed in Table 1. The integrated IR absorbance for a given band between $\tilde{\nu}_1$ and $\tilde{\nu}_2$, A_{int}, is expressed according to the Beer-Lambert law by:

$$A_{\text{int}} = \int_{\text{band}} A(\tilde{\nu})\mathrm{d}\tilde{\nu} = \int_{\text{band}} \sigma(\tilde{\nu})\ell[\mathrm{CF_3(CH_2)_xCHO}]\mathrm{d}\tilde{\nu}\,, \quad (3)$$

where $A(\tilde{\nu})$ is the absorbance at a wavenumber $\tilde{\nu}$, $\sigma(\tilde{\nu})$ is the absorption cross section at that wavenumber, and λ is the optical pathlength. The integrated absorption cross section, S_{int}, can be defined as follows:

$$S_{\text{int}} = \int_{\text{band}} \sigma(\tilde{\nu})\mathrm{d}\tilde{\nu}\,. \quad (4)$$

Thus, the expression of the Beer-Lambert law is simplified to:

$$A_{\text{int}} = S_{\text{int}}\ell[\mathrm{CF_3(CH_2)_xCHO}]\,, \quad (5)$$

S_{int} was then obtained from the linear least-squares analysis of the plots of Eq. (5). An example of such plots is presented in Fig. 2. For each band and fluorinated aldehyde, S_{int} are listed in Table 1. During the kinetic experiment an average of the aldehyde concentration extracted from all bands was taken into account in order to derive the OH rate coefficients. The aldehyde concentration measured by FTIR was usually lower than that measured from the flow rate (up to 20% difference).

2.4 Kinetic data analysis

Reactions 1 and 2 were studied under pseudo-first order conditions with fluoroaldehydes ($[\mathrm{CF_3(CH_2)_xCHO}]=(0.1-8.8)\times10^{14}$ molecule cm^{-3}) and precursor concentrations in large excess respect to the initial concentration of the oxidants. In both systems, the

ACPD
9, 24783–24814, 2009

temporal profiles of the photochemically generated oxidant can be described by the following kinetic scheme:

$$\text{Oxidant} + CF_3(CH_2)_xCHO \rightarrow \text{Products}\ k_{oxid}, \quad (6)$$

$$\text{Oxidant} + \text{Precursor} \rightarrow \text{Products}\ k_{prec}, \quad (7)$$

$$\text{Oxidant} \rightarrow \text{Loss by diffusion}\ k_{diff}, \quad (8)$$

k_{oxid} is the bimolecular rate coefficients for the reaction of Cl and OH with $CF_3(CH_2)_xCHO$, i.e., k_{Cl} and k_{OH}, respectively. In the absence of fluoroaldehyde, only Reacts. 7 and 8 are taking place, where k_{prec} is the bimolecular rate coefficient for that reaction and k_{diff} is the first-order diffusion rate coefficient of the oxidant out of the detection zone. The reaction of Cl atoms with its photochemical precursor, Cl_2, is negligible (Hutton and Wright, 1965), but the reaction of OH radicals with H_2O_2 is a significant contribution to the decay of OH concentration (Sander et al., 2006; Jiménez et al., 2004). So, under these conditions, the oxidant concentration profile should follow a simple exponential rate law:

$$[\text{Oxidant}]_t = [\text{Oxidant}]_0 \exp(-k't), \quad (9)$$

$$k' = k_{oxid}[CF_3(CH_2)_xCHO] + k_0, \quad (10)$$

where k' is the pseudo-first order rate coefficient obtained from the analysis of Eq. (9) in terms of fluorescence signal. k' ranged from 96 to 6019 s^{-1} for the $Cl+CF_3CH_2CHO$ reaction and between 226 and 8104 s^{-1} for the $Cl+CF_3CH_2CH_2CHO$ reaction. k_0 is the pseudo-first order rate coefficient recorded in the absence of fluoroaldehyde:

$$k_0 = k_{OH}[H_2O_2] + k_{diff}(OH), \quad (11)$$

$$k_0 = k_{diff}(Cl), \quad (12)$$

ACPD
9, 24783–24814, 2009

k_0 ranged from 91 to 866 s^{-1} in the case of the reactions of OH radicals and k' range was 234–2696 s^{-1} for CF_3CH_2CHO and 627–7606 s^{-1} for $CF_3CH_2CH_2CHO$. For chlorine atoms, $k_0 = k_{diff}(Cl)$ which ranged from 20 to 46 s^{-1} at p_T = 50–200 Torr of He. The bimolecular rate coefficients k_{oxid} were obtained from the slopes of the plots of k' against the fluoroaldehyde concentration (Eq. 10) or the plots of Eq. (13):

$$k' - k_0 = k_{oxid}[CF_3(CH_2)_xCHO] \quad (13)$$

Examples of $k' - k_{diff}$ and $k' - k_0$ versus $[CF_3(CH_2)_xCHO]$ plots are presented in Fig. 3a and 3b, respectively, at 298 K and total pressures between 50 and 215 Torr. At other temperatures (T = 263–371 K), k' was measured for the titled reactions at a total pressure of 100 Torr for Cl-reactions and at total pressures between 50 and 215 Torr for OH-reactions. Several examples of the plots of Eq. (13) at three different temperatures are given in Fig. 4 for the Cl and OH reactions, respectively.

Temporal profiles of the OH LIF signal were always monoexponential. In contrast, preliminary kinetic experiments showed that Cl decays in the presence of the fluoroaldehydes were biexponential. This behaviour was attributed to the regeneration of Cl via the secondary reaction:

$$CF_3(CH_2)_xCO + Cl_2 \rightarrow CF_3(CH_2)_xCOCl + Cl, \quad (14)$$

where $CF_3(CH_2)_xCO$ is the likely radical formed in the initial Cl-reaction of $CF_3(CH_2)_xCHO$. To make this secondary reaction negligible, an oxygen concentration up to 1×10^{16} molecule cm^{-3} was added to the reaction mixture through a mass flow controller. The Cl atom decay was then monoexponential, showing that the radical $CF_3(CH_2)_xCO$ reacts predominantly with O_2 under these experimental conditions.

$$CF_3(CH_2)_xCO + O_2 \rightarrow CF_3(CH_2)_xC(O)O_2. \quad (15)$$

This observation is consistent with a rate ratio $k_{(CF_3(CH_2)_xCO+O_2)}[O_2]/k_{(CF_3(CH_2)_xCO+Cl_2)}[Cl_2] \geq 50$, which can be estimated for $[O_2]/[Cl_2] = 50$ from our experimental conditions,

and taking $k_{(CF_3(CH_2)_xCO+O_2)}/k_{(CF_3(CH_2)_xCO+Cl_2)} \geq 1$ based on existing data at room temperature for $k_{(CF_3CO+O_2)}/k_{(CF_3CO+Cl_2)} \cong 1.2$ (Maricq et al., 1995; Wallington et al., 1994). On the other hand, the addition of O_2 decreased the detection sensitivity of Cl atoms, as O_2 is an efficient quencher and absorber of the fluorescence of Cl atoms. Thus, the concentration of added O_2 was limited to $\sim 1\times10^{16}$ molecule cm^{-3}. A few experiments were performed with $[O_2]\sim 2\times 1016$ molecule cm^{-3} for a limited range of aldehyde concentrations, and the obtained rate coefficients were similar to those obtained with $[O_2]\sim 1\times10^{16}$ molecule cm^{-3}. This latter concentration was considered to be suitable to prevent the $CF_3(CH_2)_xCO+Cl_2$ reaction without decreasing the detection sensitivity of Cl atoms too much.

Chemicals. Helium (UHP >99.999% from Praxair and Air Liquid) was employed as supplied. Cl_2 (99.9%, Praxair), CF_3CH_2CHO (>97%, Apollo-Scientific), and $CF_3CH_2CH_2CHO$ (95%, Apollo-Scientific) were degassed several times at 77 K before use by repeated freeze, pump, and thaw cycles. Purity of $CF_3(CH_2)_xCHO$ samples was checked by GC-MS.

3 Results and discussion

3.1 Absolute rate coefficients at 298 K and comparison with previous kinetic studies

As shown in Fig. 3, no pressure dependence of k_{Cl} and k_{OH} was observed between 50 and 215 Torr of Helium. The same trend was observed at temperatures below and above room temperature. So, weighted averages of k_{Cl} and k_{OH} are reported in Tables 2 and 3, respectively. The weighting factor was taken as the inverse of the variance of each individual measurement. Uncertainties stated in Tables 2 and 3 are only statistical errors ($\pm 2\sigma$). Systematic errors account mainly for the uncertainties in the measurement of the aldehyde concentration, since errors in the measurement of tem-

perature and pressure are much lower than 1%. Since in the Cl-kinetics aldehyde concentrations were not optically measured, an additional 20% was added to the statistical uncertainty. Thus, at room temperature the averaged rate coefficients obtained were ($\pm 2\sigma$):

$$k_{Cl}(CF_3CH_2CHO)_{298K} = (1.55 \pm 0.53) \times 10^{-11}\,cm^3\,molecule^{-1}\,s^{-1},$$
$$k_{Cl}(CF_3(CH_2)_2CHO)_{298K} = (3.39 \pm 1.38) \times 10^{-11}\,cm^3\,molecule^{-1}\,s^{-1},$$
$$k_{OH}(CF_3CH_2CHO)_{298K} = (2.59 \pm 0.50) \times 10^{-12}\,cm^3\,molecule^{-1}\,s^{-1},$$
$$k_{OH}(CF_3(CH_2)_2CHO)_{298K} = (1.28 \pm 0.24) \times 10^{-11}\,cm^3\,molecule^{-1}\,s^{-1}.$$

As pointed out in the Introduction section, only a few measurements of k_{Cl} and k_{OH} for CF_3CH_2CHO are found in the literature at room temperature (Hurley et al., 2005; Kelly et al., 2005; Sellevåg et al., 2004b). These previous studies were performed almost exclusively by relative methods. Therefore, k_{Cl} measured in this work represents the first absolute value of that rate coefficient, as far as we know. Furthermore, our kinetic study on the Cl and OH reactions with $CF_3(CH_2)_2CHO$ constitutes the first rate coefficients reported for this partially fluorinated aldehyde.

Table 4 summarizes our results at 298 K together with those previously reported for the reaction of Cl and OH with CF_3CH_2CHO. As it can be seen in the table, the absolute rate coefficient $k_{Cl}(CF_3CH_2CHO)$ obtained in this work agrees with that of Hurley et al. (2005). Some discrepancy observed in $k_{Cl}(CF_3CH_2CHO)$ in previous relative studies can be related with the use of different reference compounds, as discussed by Hurley et al. (2005). Regarding the OH-rate coefficient for CF_3CH_2CHO, Kelly et al. (2005) reported the only absolute k_{OH} data employing the PLP/LIF technique, which is in agreement with the value reported in this paper and the relative one from Hurley et al. (2005), who used ethane and ethene as reference compounds. In this case, the discrepancy between the relative studies of Sellevåg et al. (2004b) and Hurley et al. (2005) remains unclear.

Room temperature k_{Cl} and k_{OH} for fluorinated aldehydes and the corresponding non-fluorinated aldehydes are compared in Tables 5 and 6, respectively. As it can be seen, a deactivation effect of CF_3 group is clearly observed in both set of reactions. The rate ratio $k(CF_3(CH_2)_xCHO)/k(CH_3(CH_2)_xCHO)$ ranges from 0.02 for the reaction of CF_3CHO with Cl atoms to 0.51 for the OH-reaction with $CF_3(CH_2)_2CHO$. Also, as Tables 5 and 6 show, k_{Cl} and k_{OH} significantly increase with the length of the hydrocarbon chain, compared to the slight increase observed for the corresponding reactions with non-fluorinated aldehydes (Atkinson et al., 2006). Rate ratios $k(CF_3(CH_2)_xCHO)/k(CF_3(CH_2)_{x-1}CHO)$ range from ca. 2 to 9, while $k(CH_3(CH_2)_xCHO)$ is more than 20% larger that $k(CH_3(CH_2)_{x-1}CHO)$. The enhancement in the reactivity of higher fluorinated aldehydes can be explained by a lower influence of the deactivation effect of -CF_3 group, which favours the H-atom abstraction from the aldehydic group. Mechanistic studies on the Cl-reaction with CF_3CH_2CHO confirmed that the main reaction pathway is H-atom abstraction from aldehydic group (Hurley et al., 2005). No product studies on the Cl and OH-reactions with $CF_3(CH_2)_2CHO$ has been reported, as far as we know.

3.2 Absolute rate coefficients k_{Cl} and k_{OH} as a function of temperature

A summary of the absolute second-order rate coefficients for the reactions of Cl and OH with the studied aldehydes at all temperatures is given in Tables 2 and 3, respectively. The influence of temperature over the 263–371 K range on k_{Cl} and k_{OH} can be seen in the pseudo-first order plots given in Fig. 4 for each reaction and the corresponding Arrhenius plots presented in Fig. 5. The temperature dependence observed for the Cl- and OH-reactions with CF_3CH_2CHO was slightly positive, i.e. the rate coefficients slightly increase with temperature:

$$k_{Cl}(CF_3CH_2CHO) = (4.4 \pm 1.0) \times 10^{-11} \exp\{-(316 \pm 68)/T\} \text{cm}^3 \text{molecule}^{-1} \text{s}^{-1},$$
$$k_{OH}(CF_3CH_2CHO) = (7.8 \pm 2.2) \times 10^{-12} \exp\{-(314 \pm 90)/T\} \text{cm}^3 \text{molecule}^{-1} \text{s}^{-1}.$$

This behaviour was also observed for the reaction of Cl atoms with $CF_3(CH_2)_2CHO$:

$$k_{Cl}(CF_3(CH_2)_2CHO) = (2.9 \pm 0.7) \times 10^{-10} \exp\{-(625 \pm 80)/T\} cm^3 molecule^{-1} s^{-1}.$$

In contrast, the corresponding reaction with OH radicals seems to proceed with no energy barrier, within the experimental errors:

$$k_{OH}(CF_3(CH_2)_2CHO) = (9.0 \pm 2.9) \times 10^{-12} \exp\{(92 \pm 104)/T\} cm^3 molecule^{-1} s^{-1}.$$

In this case, we recommend the weighted average of k_{OH} between 263 and 358 K:

$$k_{OH}(CF_3(CH_2)_2CHO) = (1.21 \pm 0.10) \times 10^{-11} cm^3 molecule^{-1} s^{-1}.$$

A summary of the Arrhenius parameters, E_a/R and A, and the room temperature rate coefficients for the reactions of $CF_3(CH_2)_xCHO$ and $CH_3(CH_2)_xCHO$ (x=0, 1, and 2) with Cl and OH is presented in Tables 5 and 6, respectively. As Table 6 shows, a positive E_a/R was also reported for the OH-reaction with CF_3CHO (Laverdet et al., 1993). In the case of the reaction with Cl atoms no kinetic studies were found as a function of temperature. Positive activation energies are usually indicative that the major reaction pathway proceeds via a H-atom abstraction mechanism (Atkinson and Arey, 2003). In fact, product studies on Cl- and OH-reactions with CF_3CHO (Sellevåg et al., 2004b; Sulbaek Andersen et al., 2004) and CF_3CH_2CHO (Hurley et al., 2005) confirm that the abstraction of the hydrogen atom from the CHO group is the major reaction pathway, as mentioned above. In contrast, while $k_{Cl}(CH_3CHO)$ did not show a temperature dependence (Atkinson et al., 2006), most of the reactions with non-fluorinated aldehydes exhibit a negative temperature dependence and similar E_a/R factors. Negative temperature dependence is frequently associated with the formation of a long-lived addition complex before the hydrogen abstraction by Cl atoms or OH radicals, as suggested by Smith and Ravishankara (2002) for oxygenated organic compounds.

ACPD
9, 24783–24814, 2009

3.3 Tropospheric lifetimes of $CF_3(CH_2)_xCHO$

Global tropospheric lifetimes of $CF_3(CH_2)_xCHO$ due to homogeneous reactions with OH radicals and Cl atoms, τ_{homog}, were calculated by using the rate coefficient k_{OH} and k_{Cl} and a 24 h average oxidant concentration in the atmosphere of 1×10^6 radical cm^{-3} for OH (Krol et al., 1998) and 10^3 atom cm^{-3} for Cl (Sighn et al., 1996). Under these conditions, τ_{OH} for CF_3CH_2CHO was estimated to be 4 days at the surface and 6 days in the upper troposphere. In contrast, a constant τ_{OH} for $CF_3(CH_2)_2CHO$ of one day along the troposphere is reported here. Concerning τ_{Cl} for $CF_3(CH_2)_xCHO$ were estimated to be more than one year. Globally, the tropospheric removal of both fluorinated aldehydes is dominated by the reaction with OH radicals, i. e., τ_{homog} is almost equal to τ_{OH}.

In coastal areas and some industrialized zones, the Cl concentration can reach a peak value of 1.3×10^5 atom cm^{-3} (Spicer et al., 1998) at dawn, where [OH] and solar actinic flux are very low. Under these circumstances, Cl atoms is the responsible of the removal of $CF_3(CH_2)_xCHO$. At night the atmospheric degradation of fluorinated aldehydes is expected to be of minor importance, since lifetimes due to the reaction with NO_3 radicals are likely to be much longer than several days.

Other degradation routes to take into account in order to evaluate the atmospheric lifetimes of these $CF_3(CH_2)_xCHO$ can be UV photolysis in the actinic region (λ>290 nm) and aqueous-phase atmospheric degradation.

The atmospheric lifetime of CF_3CH_2CHO with respect to UV photolysis has been estimated to be longer than 15 days (Sellevåg et al., 2004b; Chiappero et al., 2006). If the photolysis quantum yield (Φ_λ) of the fluorinated aldehyde depends on total pressure, the photolysis of CF_3CH_2CHO could be more important than reported at higher altitudes in the troposphere. As far as we know, no photodegradation study on $CF_3(CH_2)_2CHO$ has been reported. Thus, a similar photolysis rate to CF_3CH_2CHO was assumed in this work for 4,4,4-trifluorobutanal. Further studies on the pressure dependence of both fluoroaldehydes are needed in order to better evaluate this removal

ACPD
9, 24783–24814, 2009

process along the troposphere.

Scarce information is available for the aqueous-phase degradation of fluorinated aldehydes. The atmospheric lifetime due to the water phase removal depends on the Henry's law coefficients $k_{H,cp}$ (=C/p, in Matm^{-1}) and the hydrolysis rate coefficients, k_{hyd}. For some fluorinated oxygenated compounds have been compiled by Sander (1999). $k_{H,cp}$ ranges from 3 Matm^{-1} for FCHO to 160 Matm^{-1} for $CHF_2CF_2CH_2OH$, which indicate that these species will remain predominately in the liquid phase. No measurements of $k_{H,cp}$ have been found in the literature for other fluorinated aldehydes rather than FCHO. Based upon the air-water partition coefficients given above and assuming an annual rainfall rate of 580 mmyr^{-1}, as in previous works (Jiménez et al., 2009), the lifetime of $CF_3(CH_2)_xCHO$ with respect to wet deposition can be assessed to be up to 300 years or longer in the free and upper troposphere. Heterogeneous kinetics on these fluorinated aldehydes has not been studied, but it is expected that the uptake of $CF_3(CH_2)_xCHO$ on or into the aqueous component of cloud/fog droplets or aqueous aerosol particles is not likely to be an important atmospheric sink for these compounds. However, further studies are needed in order to better evaluate this degradation route, since it can be a source of fluorinated acids, $CF_3(CH_2)_xC(O)OH$, in the atmosphere.

In conclusion, the removal of CF_3CH_2CHO by UV photolysis in troposphere might not be negligible respect to that by OH radicals. However, the removal of $CF_3(CH_2)_2CHO$ by OH radicals might be its major atmospheric sink. Therefore, the products of their reactions with OH radicals and UV photolysis may exert a great influence on the air quality. Similarly to Cl atoms (Hurley et al., 2005), major products of the OH-reactions with CF_3CH_2CHO and $CF_3(CH_2)_2CHO$ are likely to be the corresponding fluorinated acids and CF_3CHO and CF_3CH_2CHO, respectively, in clean atmospheres. Like CF_3CHO (Chiappero et al., 2006), UV photolysis products of $CF_3(CH_2)_xCHO$ at 308 nm (near the absorption maximum) are likely to be those from the radical channel, yielding formyl radical (HCO) and fluoroalkyl radical, $CF_3(CH_2)_x$. Further reaction of all the species formed in such degradation processed would greatly contribute to smog formation. In

ACPD
9, 24783–24814, 2009

this sense, the role of the Cl reactions in ozone formation, for example, should be considered since previous studies suggest that chlorine radical chemistry enhances ozone formation in different areas. Thus for example, the model used by Knipping and Dabdub (2003) with an explicit treatment of sea-salt aerosol multiphase chemistry, showed that Cl-initiated VOCs oxidation can increase morning ozone concentrations by as much as 12 ppb in coastal regions. On the other hand, the observation that ozone concentrations are higher on weekends than on weekdays, despite lower atmospheric levels of ozone precursors on weekends, has been long recognized as the weekend effect. Cohan et al. (2008) carried out a modelling study observing important processes previously neglected by other researchers, including the impacts of heterogeneous chlorine chemistry on the weekend effect, particularly in coastal regions. Finally, additional photochemical studies would be needed to better evaluate the tropospheric impact of $CF_3(CH_2)_xCHO$.

4 Conclusions

In this paper, we provide for the first time a detailed study on the temperature dependence of the absolute rate coefficients k_{Cl} and k_{OH} in the gas phase between 263 and 371 K. Activation energies (E_a) and pre-exponential factors (A) of reactions 1 and 2 have been reported here for the first time. Similar slightly positive activation energies of 2.6 kJ/mol were obtained for the reactions of CF_3CH_2CHO with Cl and OH. The observed kinetic behaviour of $CF_3(CH_2)_2CHO$ with respect to temperature seems to be different for both radicals. E_a(Cl) is 5.2 kJ/mol, while the OH-reaction has no energy barrier, within the error limits. We can observe an enhancement in the reactivity of higher fluorinated aldehydes by comparison with similar aldehydes possibly by a lower influence of the deactivation effect of CF_3 group, which seems to favour the H-atom abstraction from the aldehydic group. The evaluation of the atmospheric lifetimes of the secondary pollutant $CF_3(CH_2)_xCHO$ under global and specific conditions indicates that are rapidly degradated in the troposphere. That implies that other pollutants, such as smaller fluorinated aldehydes, and free radicals

ACPD
9, 24783–24814, 2009

are generated, which can contribute to the air pollution. Also, the atmospheric degradation of these partially fluorinated aldehydes can be a source of $CF_3(CH_2)_xC(O)OH$ in the troposphere. Lastly an important degradation process to be taken into account is the UV photolysis of $CF_3(CH_2)_xCHO$ which seems to be an important removal route for these species. Future studies on the photolysis of $CF_3(CH_2)_xCHO$ in the actinic region are needed to better quantify this removal process. Plots of the Beer-Lambert's law for CF_3CH_2CHO and $CF_3(CH_2)_2CHO$ at 185 nm (Fig. 1S http://www.atmos-chem-phys-discuss.net/9/24783/2009/acpd-9-24783-2009-supplement.pdf) and at several wavenumber ranges (Fig. 3S http://www.atmos-chem-phys-discuss.net/9/24783/2009/acpd-9-24783-2009-supplement.pdf) are available in the supplementary information. Also an example of the recorded infrared spectrum at 298 K for each species is presented in Fig. 2S http://www.atmos-chem-phys-discuss.net/9/24783/2009/acpd-9-24783-2009-supplement.pdf.

Acknowledgements. The authors thank the Spanish Ministerio de Ciencia e Innovación (MICINN) and the Consejería de Ciencia y Tecnología (Junta de Comunidades de Castilla-La Mancha) for supporting this research under projects CGL2007-61835/CLI and PCI08-0123-0381, respectively. M. Antiñolo also wishes to thank to MICINN for providing her a grant.

References

Albaladejo, J., Ballesteros, B., Jiménez, E., Martín, P., and Martínez, E.: A PLP-LIF kinetic study of the atmospheric reactivity of a series of C_4-C_7 saturated and unsaturated aliphatic aldehydes with OH, Atmos. Environ., 36, 3231–3239, 2002.

Albaladejo, J., Notario, A., Cuevas, C. A., Ballesteros, B., and Martínez, E.: A Pulsed laser photolysis-resonance fluorescence kinetic study of the atmospheric Cl atom-initiated oxidation of propene and a series of 3-halopropenes at room temperature, J. Atmos. Chem., 45, 35–50, 2003.

Atkinson, R. and Arey, J.: Atmospheric degradation of volatile organic compounds, Chem. Rev., 103, 4605–4638, 2003.

Atkinson, R., Cox, R. A., Lesclaux, R., Niki, H., and Zellner, R.: Degradation Mechanisms, in:

Scientific Assessment of Stratospheric Ozone, Vol. 2, Global Ozone research and Monitoring Project – Report No. 20; World Meteorological Organization: Geneva, Switzerland, 1989.
Atkinson, R., Baulch, D. L., Cox, R. A., Crowley, J. N., Hampson, R. F., Hynes, R. G., Jenkin, M. E., Rossi, M. J., Troe, J., and IUPAC Subcommittee: Evaluated kinetic and photochemical data for atmospheric chemistry: Volume II – gas phase reactions of organic species, Atmos. Chem. Phys., 6, 3625–4055, 2006, http://www.atmos-chem-phys.net/6/3625/2006/.
Atkinson, R., Baulch, D. L., Cox, R. A., Crowley, J. N., Hampson, R. F., Hynes, R. G., Jenkin, M. E., Rossi, M. J., Troe, J., and Wallington, T. J.: Evaluated kinetic and photochemical data for atmospheric chemistry: Volume IV – gas phase reactions of organic halogen species, Atmos. Chem. Phys., 8, 4141–4496, 2008, http://www.atmos-chem-phys.net/8/4141/2008/.
Chandra, A. K., Uchimaru, T., and Sugie, M.: Kinetics of hydrogen abstraction reactions of CF_3CHO, CF_2ClCHO, $CFCl_2CHO$ and CCl_3CHO with OH radicals: An ab initio atudy, Phys. Chem. Chem. Phys., 3, 3961–3966, 2001.
Chiappero, M. S., Malanca, F. E., Argüello, G. A., Wooldridge, S. T., Hurley, M. D., Ball, J. C., Wallington, T. J., Waterland, R. L., and Buck, R. C.: Atmospheric chemistry of perfluoroaldehydes ($C_xF_{2x+1}CHO$) and fluorotelomer aldehydes ($C_xF_{2x+1}CH_2CHO$): Quantification of the important role of photolysis, J. Phys. Chem. A, 110, 11 944-11 953, 2006.
Cohan, A., Chang, W., Carreras-Sospedra ,M., Dabdub, D.: Influence of sea-salt activated chlorine and surface-mediated renoxification on the weekend effect in the South Coast Air Basin of California, Atmos. Environ., 42, 3115–3129, 2008.
Cuevas, C. A., Notario, A., Martinez, E., and Albaladejo, J.: Temperature-dependence study of the gas-phase reactions of atmospheric Cl atoms with a series of aliphatic aldehydes, Atmos. Environ., 40, 3845–3854, 2006.
Dóbé, S., Khachatryan, L. A., and Berces, T.: Kinetics of reactions of hydroxyl radicals with a series of aliphatic aldehydes, Ber. Bunsen-Ges. Phys. Chem., 93, 847–852, 1989.
Hutton, E. and Wright, M. Photoemissive and recombination reactions of atomic chlorine, Trans. Faraday Soc., 61, 78–89, 1965.
Hurley, M. D., Wallington, T. J., Andersen, M. P S., Ellis, D. A., Martin, J. W., and Mabury, S. A.: Atmospheric chemistry of fluorinated alcohols: Reaction with Cl atoms and OH radicals and atmospheric lifetimes, J. Phys. Chem. A, 108, 1973–1979, 2004.
Hurley, M. D., Misner, J. A., Ball, J. C., Wallington, T. J., Ellis, D. A., Martin, J. W., Mabury, S. A., and Sulbaek Andersen, M. P.: Atmospheric chemistry of $CF_3CH_2CH_2OH$: kinetics, mechanisms and products of Cl atom and OH radical initiated oxidation in the presence and

absence of NO_x, J. Phys. Chem. A, 109, 9816–9826, 2005.
Jiménez, E., Gierczak, T., Burkholder, J. B., Stark, H., and Ravishankara, A. R.: Reaction of OH with HO_2NO_2 (Peroxynitric Acid): Rate coefficients between 218 and 335 K and product yields at 298 K, J. Phys. Chem. A, 108, 1139–1149, 2004.
Jiménez, E., Lanza, B., Garzón. A., Ballesteros, B., and Albaladejo, J.: Atmospheric degradation of 2-butanol, 2-methyl-2-butanol, and 2,3-dimethyl-2-butanol: OH kinetics and UV absorption cross sections, J. Phys. Chem. A, 109, 10 903–10 909, 2005.
Jiménez, E., Lanza, B., Martínez, E., and Albaladejo, J.: Daytime tropospheric loss of hexanal and *trans*-2-hexenal: OH kinetics and UV photolysis, Atmos. Chem. Phys., 7, 1565–1574, 2007, http://www.atmos-chem-phys.net/7/1565/2007/.
Jiménez, E., Lanza, B., Antiñolo, M., and Albaladejo, J.: Photooxidation of leaf-wound oxygenated compounds, 1-penten-3-ol, (*Z*)-3-hexen-1-ol, and 1-penten-3-one, initiated by OH radicals and sunlight, Environ. Sci. Technol., 43, 1831–1837, 2009.
Kelly, T., Bossoutrot, V., Magneron, I., Wirtz, K., Treacy, J., Mellouki, A., Sidebottom, H., and Le Bras, G.: A kinetic and mechanistic study of the reactions of OH radicals and Cl atoms with 3,3,3-trifluoropropanol under atmospheric conditions, J. Phys. Chem. A, 109, 347–355, 2005.
Knipping, E. M. and Dabdub, D.: Impact of chlorine emissions from sea-salt aerosol on coastal urban ozone, Environ. Sci. Tech., 37, 275–284, 2003.
Krol, M., van Leeuwen, P. J., and Lelieveld, J.: Global OH Trend Inferred from Methylchloroform Measurements, J. Geophys. Res. Atmos., 103, 10 697–10 711, 1998.
Lanza, B., Jiménez, E., Ballesteros, B., and Albaladejo, J.: Absorption cross section determination of biogenic C_5 aldehydes in the actinic region, Chem. Phys. Lett., 454, 184–189, 2008.
Laverdet, G., Le Bras, G., MacLeod, H., Poulet, G., Teton, S., Scollard, D. J., Treacy, J. J., and Sidebottom, H. H.: Laser photolysis-resonance fluorescence investigation of the reactions of hydroxyl radicals with CCl_3CHO and CF_3CHO as a function of temperature, Proc. SPIE-Int. Soc. Opt. Eng., 1715, 100–112, 1993.
Maricq, M. M., Szente, J. J., Khitrov, G. A., Dibble, T. S., and Francisco, J. S.: CF_3CO dissociation kinetics, J. Phys. Chem. A., 99, 11 875–11 882, 1995.
Ravishankara, A. R., Turnipseed, A. A., Jensen, N. R., Barone, S., Mills, M., Howard, C. J., and Solomon, S.: Do hydrofluorocarbons destroy stratospheric ozone?, Science, 263, 71–75, 1994.

Sander, R.: Compilation of Henry's law constants for inorganic and organic species of potential importance in environmental chemistry, 1999. Available at http://www.henrys-law.org.

Sander, S. P., Friedl, R. R., Golden, D. M., Kurylo, M. J., Huie, R. E., Orkin, V. L., Moortgat, G. K., Ravishankara, A. R., Kolb, C. E., Molina, M. J., and Finlayson-Pitts, B. J.: Chemical kinetics and photochemical data for use in Atmos. studies, Vol. 02-25, Evaluation number 14, Jet Propulsion Laboratory, California Institute of Technology, Pasadena, CA, 2006.

Sellevåg, S. R., Nielsen, C. J., Sovde, O. A., Myhre, G., Sundet, J. K., Stordal, F., and Isaksen, I. S.: Atmospheric gas-phase degradation and global warming potentials of 2-fluoroethanol, 2,2-difluoroethanol, and 2,2,2-trifluoroethanol, Atmos. Environ., 38, 6725–6735, 2004a.

Sellevåg, S. R., Kelly, T., Sidebottom, H., Nielsen, C. J.: A study of the IR and UV-Vis absorption cross-sections, photolysis and OH-initiated oxidation of CF_3CHO and CF_3CH_2CHO, Phys. Chem. Chem. Phys., 6, 1243–1252, 2004b.

Singh, H. B., Thakur, A. N., Chen, Y. E., and Kanakidou M.: Tetrachloroethylene as an indicator of low Cl atom concentrations in the troposphere, Geophys. Res. Lett., 23, 1529–1532, 1996.

Smith, I. W. M. and Ravishankara, A. R.: Role of hydrogen-bonded intermediates in the bimolecular reactions of the hydroxyl radical, J. Phys. Chem. A, 106, 4798–4807, 2002.

Spicer, C. W., Chapman, E. G., Finlayson-Pitt, B. J., Plastridge, R. A., Hubbe, J. M., Fast, J. D., and Berkowitz, C. M.: Unexpectedly high concentrations of molecular chlorine in coastal air, Nature, 394, 353–356, 1998.

Sulbaek Andersen, M. P., Nielsen, O. J., Hurley, M. D., Ball, J. C., Wallington, T. J., Stevens, J. E., Martin, J. W., Ellis, D. A., and Mabury, S. A.: Atmospheric Chemistry of n-$C_xF_{2x+1}CHO$ (x=1,3,4): Reaction with Cl atoms, OH radicals and IR spectra of $C_xF_{2x+1}C(O)O_2NO_2$, J. Phys. Chem. A, 108, 5189–5196, 2004.

Wallington, T. J. and Hurley, M. D.: A Kinetic study of the reaction of chlorine and fluorine atoms with CF_3CHO at 295±2K, Int. J. Chem. Kinet., 25, 819–824, 1993.

Wallington, T. J., Hurley, M. D., Nielsen, O. J., and Sehested, J.: Atmospheric chemistry of CF_3CO_x, radicals: Fate of CF_3CO radicals, the UV absorption spectrum of $CF_3C(O)O_2$ radicals, and kinetics of the reaction $CF_3C(O)O_2+NO \rightarrow CF_3C(O)O+NO_2$, J. Phys. Chem. A, 98, 5686–5694, 1994.

Waterland, R. L., Hurley, M. D., Misner, J. A., Wallington, T. J., Melo, S. M. L., Strong, K., Dumoulin, R., Castera, L., Stock, N. L., and Mabury, S. A.: Gas phase UV and IR absorption spectra of $CF_3CH_2CH_2OH$ and $F(CF_2CF_2)_xCH_2CH_2OH$ (x=2,3,4), J. Fluor. Chem., 126, 1288–1296, 2005.

ACPD

9, 24783–24814, 2009

Table 1. Integrated absorption cross sections, S_{int}, for the four bands employed in the determination of fluorinated aldehyde concentrations.

Fluorinated aldehyde	$\tilde{\nu}_1-\tilde{\nu}_2$ Band (cm^{-1})	$(S_{int}\pm 2\sigma)\times 10^{17}$ ($cm\,molecule^{-1}$)
CF_3CH_2CHO	1112–1214	1.31±0.04
	1213–1312	1.11±0.06
	1307–1382	0.51±0.11
	1731–1776	0.44±0.02
$CF_3(CH_2)_2CHO$	1093–1198	1.84±0.01
	1202–1287	0.93±0.04
	1287–1339	0.80±0.03
	1715–1824	0.70±0.04

ACPD
9, 24783–24814, 2009

Table 2. Summary of experimental conditions and the obtained bimolecular rate coefficients for the reaction of Cl in the studied temperature range.

Fluorinated aldehyde	T (K)	p_T (Torr)	$[CF_3(CH_2)_xCHO]$ (10^{13} molecule cm^{-3})	$(k_{Cl}\pm2\sigma)\times10^{11}$ (cm^3 molecule^{-1} s^{-1})
CF_3CH_2CHO	268	100	0.92–8.0	1.37±0.10
	278	100	0.80–7.5	1.42±0.10
	288	100	0.79–7.7	1.38±0.11
	297	50–200	0.39–15	1.55±0.22
	316	100	1.8–17	1.67±0.38
	331	100	1.6–15	1.75±0.32
	351	100	1.8–12	1.80±0.36
	371	100	1.4–13	1.84±0.15
$CF_3(CH_2)_2CHO$	268	100	1.3–11	2.85±0.45
	278	100	1.5–13	2.98±0.20
	288	100	1.3–11	3.20±0.14
	298	50–200	0.75–21	3.39±0.70
	316	100	1.2–11	4.05±0.46
	331	100	1.2–10	4.60±0.24
	351	100	1.3–11	4.79±0.74
	371	100	1.2–10	5.13±0.41

ACPD
9, 24783–24814, 2009

Table 3. Summary of experimental conditions and the obtained rate coefficients for the reaction of OH with the studied compounds in the range of temperature studied.

Fluorinated aldehyde	T (K)	p_T (Torr)	$[CF_3(CH_2)_xCHO]$ (10^{14} molecule cm^{-3})	($k_{OH}\pm2\sigma$)$\times10^{12}$ (cm^3 molecule^{-1} s^{-1})
CF_3CH_2CHO	263	67–76	0.19–3.2	2.59±0.36
	270	74–79	0.10–4.2	2.24±1.04
	278	68–79	0.21–5.3	2.34±0.29
	287	61–99	0.10–4.6	2.71±0.55
	298	55–215	0.30–8.5	2.59±0.50
	308	59–94	0.10–8.8	2.93±0.80
	323	63–93	0.37–8.1	2.94±0.40
	338	60–98	0.10–6.5	3.04±0.55
	358	68–98	0.48–6.1	3.29±0.23
$CF_3(CH_2)_2CHO$	263	74–78	0.31–5.8	12.8±1.8
	270	69–81	0.30–5.2	13.1±1.4
	278	74–81	0.27–2.0	12.2±1.5
	287	70–82	0.28–5.08	12.6±1.4
	298	51–204	0.34–4.9	12.8±1.6
	308	51–71	0.28–3.8	13.1±1.3
	323	62–92	0.43–3.9	11.9±0.2
	338	57–88	0.47–3.4	12.3±0.8
	358	66–81	0.55–4.0	12.5±1.2

ACPD
9, 24783–24814, 2009

Table 4. Summary of the absolute second-order rate coefficients obtained in this work at 298 K together with those previously reported in the literature for the reaction of Cl atoms and OH radicals.

Fluoroaldehyde	$k_{Cl} \times 10^{11}$ ($cm^3 molecule^{-1} s^{-1}$)	Technique[a]	Reference	$k_{OH} \times 10^{12}$ ($cm^3 molecule^{-1} s^{-1}$)	Technique[a]	Reference
CF_3CH_2CHO	1.55±0.53	PLP/RF	This work	2.59±0.50	PLP/LIF	This work
	1.81±0.27	RR/FTIR	Hurley et al. (2005)	2.57±0.44	RR/FTIR	Hurley et al. (2005)
	2.57±0.04	RR/GC-FID and FTIR	Kelly et al. (2005)	2.96±0.04	PLP/LIF	Kelly et al. (2005)
				3.6±0.3	RR/GC-FID and FTIR	Sellevåg et al. (2004b)
$CF_3(CH_2)_2CHO$	3.39±1.38	PLP/RF	This work	12.8±2.4	PLP/LIF	This work

[a] RR, relative rate; GC-FID, Gas chromatography coupled to Flame Ionization Detection.

Table 5. Summary of the Arrhenius parameters for the reaction of Cl atoms with the studied aldehydes obtained in this work along with those found in the literature for other fluorinated aldehydes and non-fluorinated aldehydes.

Aldehyde	$k_{Cl}(T=298K)\times10^{11}$ (cm^3 $molecule^{-1}$ s^{-1})	$A\times10^{11}$ (cm^3 $molecule^{-1}$ s^{-1})	E_a/R (K)
CF_3CHO	0.18[a]	no data	no data
CF_3CH_2CHO	1.55±0.53[b]	4.4±1.0[b]	316±68[b]
$CF_3CH_2CH_2CHO$	3.39±1.38[b]	29±7[b]	625±80[b]
CH_3CHO	8.00[c]	–	–
CH_3CH_2CHO	11.0[d]	24.1[d]	−453.4[d]
$CH_3CH_2CH_2CHO$	13.8[d]	30.9[d]	−446.2[d]

[a] Wallington and Hurley (1993)
[b] This work, uncertainties stated in the text
[c] Atkinson et al. (2006), k_{Cl} independent of temperature
[d] Cuevas et al. (2006)

ACPD
9, 24783–24814, 2009

Table 6. Summary of the Arrhenius parameters for the reactions of OH radicals with the studied aldehydes obtained in this work along with those found in the literature for other fluorinated aldehydes and non-fluorinated aldehydes.

Aldehyde	$k_{OH}(T=298K)\times10^{12}$ (cm^3 $molecule^{-1}$ s^{-1})	$A\times10^{11}$ (cm^3 $molecule^{-1}$ s^{-1})	E_a/R (K)
CF_3CHO		1.16[b]	349[b]
	0.58[a]	0.35±0.10[c]	488±57[c]
		0.15[d]	855[d]
CF_3CH_2CHO	2.59[e]	0.78±0.22[e]	314±90[e]
$CF_3CH_2CH_2CHO$	12.2[e]	1.06±0.24[e]	−92±104[e]
CH_3CHO	15.0[f]	0.44[f]	−365[f]
CH_3CH_2CHO	20.0[f]	0.51[f]	−405[f]
$CH_3CH_2CH_2CHO$	24.0[f]	0.60[f]	−410[f]

[a] Atkinson et al. (2008)
[b] Dóbé et al. (1989), at low pressure
[c] Laverdet et al. (1993)
[d] Chandra et al. (2001), ab initio calculations
[e] This work
[f] Atkinson et al. (2006)

ACPD
9, 24783–24814, 2009

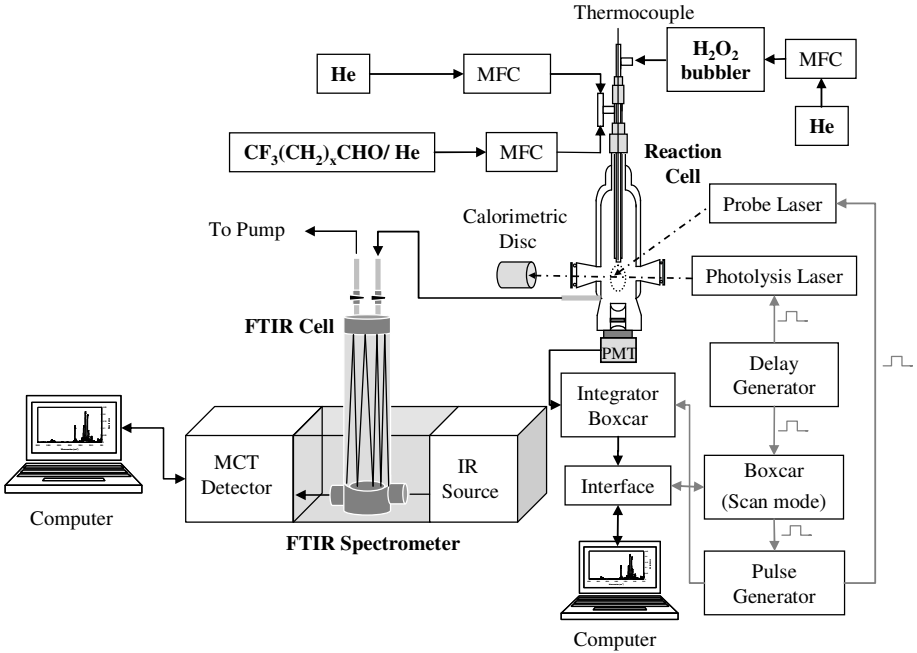

Fig. 1. Experimental set-up for the on-line measurement of the concentration of $CF_3(CH_2)_xCHO$ by FTIR spectroscopy during the OH-kinetic experiments. MFC: mass flow controller.

ACPD
9, 24783–24814, 2009

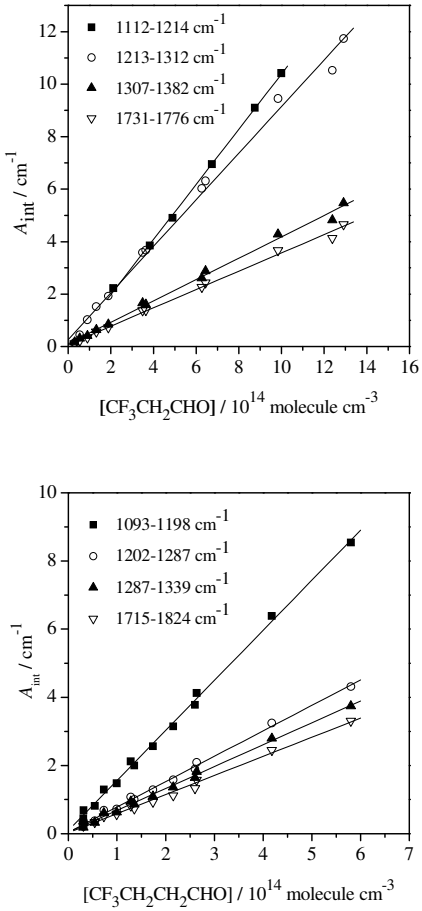

Fig. 2. Plots of the Beer-Lambert law to obtain the integrated absorption cross sections, S_{int}, for CF_3CH_2CHO and $CF_3CH_2CH_2CHO$.

ACPD
9, 24783–24814, 2009

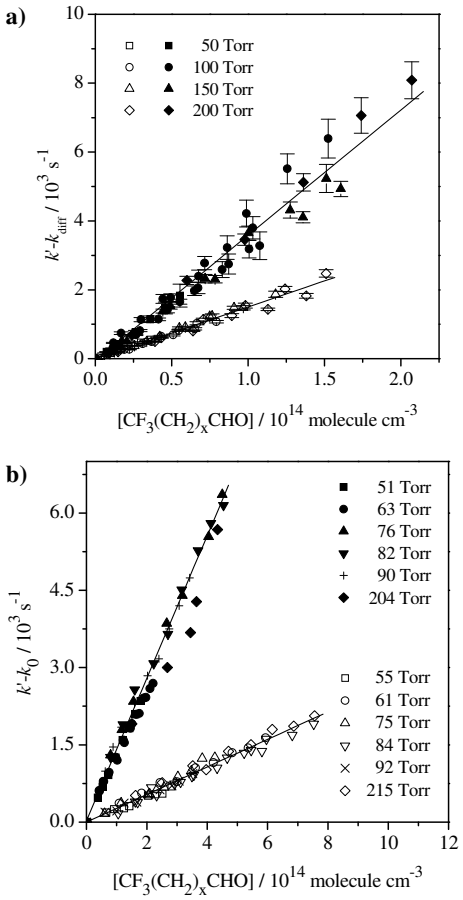

Fig. 3. Examples of the pseudo-first order plots at room temperature for **(a)** Cl reactions and **(b)** OH reactions with CF_3CH_2CHO (white symbols) and $CF_3(CH_2)_2CHO$ (black symbols).

ACPD
9, 24783–24814, 2009

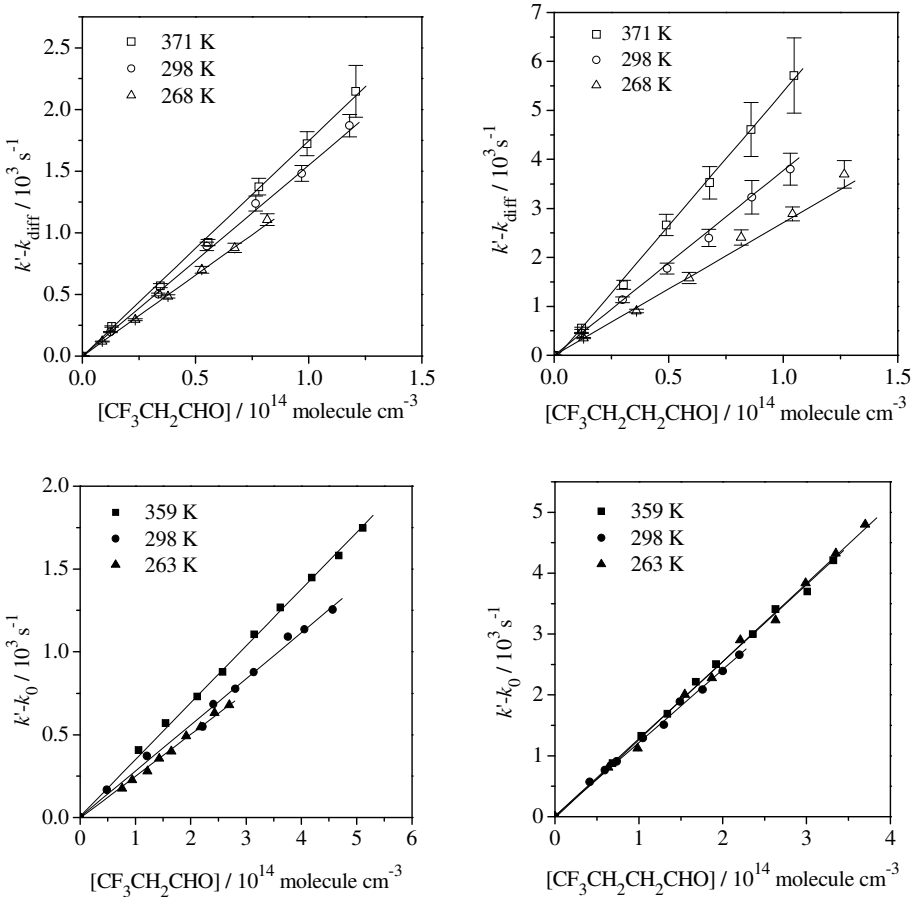

Fig. 4. Examples of the plots of $k'-k_{diff}$ (for Cl reactions) and $k'-k_0$ (for OH reactions) versus the concentration of aldehydes studied in this work at several temperatures. Solid lines are obtained from the least-squares analysis of the data.

ACPD
9, 24783–24814, 2009

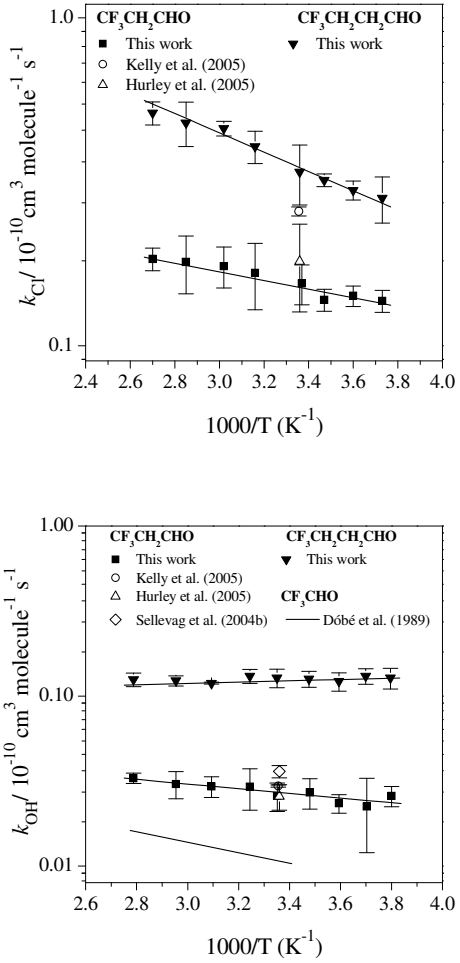

Fig. 5. Arrhenius plot of the experimental results obtained. The error bars of the individual points are $\pm 2\sigma$.

ACPD
9, 24783–24814, 2009